International Journal of Mechanical, Industrial and Aerospace Sciences
ISSN: 2517-9950
Vol:9, No:3, 2015

A Simple Device for in-situ Direct Shear and Sinkage Tests

A. Jerves, H. Ling, J. Gabaldon, M. Usoltceva, C. Cousté, A. Agarwal, R. Hurley, J. Andrade

Abstract—This work introduces a simple device designed to perform in-situ direct shear and sinkage tests on granular materials as sand, clays, or regolith. It consists of a box nested within a larger box. Both have open bottoms, allowing them to be lowered into the material. Afterwards, two rotating plates on opposite sides of the outer box will rotate outwards in order to clear regolith on either side, providing room for the inner box to move relative to the plates and perform a shear test without the resistance of the surrounding soil. From this test, Coulomb parameters, including cohesion and internal friction angle, as well as, Bekker parameters can be inferred. This device has been designed for a laboratory setting, but with few modifications, could be put on the underside of a rover for use in a remote location. The goal behind this work is to ultimately create a compact, but accurate measuring tool to put onto a rover or any kind of exploratory vehicle to test for regolith properties of celestial bodies.

Keywords—Simple shear, friction angle, Bekker parameters, device, regolith.

I. Introduction

CURRENTLY, the standard method for testing shear strength from a remote location, such as, on a rover, as described in [1], is to use a component of the wheel itself. The advantage here is that it takes up no space on the rover's body. However, testing with the wheel generates noisy data, and causes a loss of cohesion within the soil. Therefore, great efforts are required in an attempt to recover an accurate data and infer cohesion. The advantage of the device herein described is its compact nature and low requirement of energy. Although, it is slightly less space efficient, the nature of the data that can be obtained and inferred from the mentioned device is crucial for unraveling the geological history, overcoming exploratory difficulties, landing vehicles, and developing any kind of infrastructure on celestial bodies.

II. Experimental Setup

The direct shear test [6] yields the Mohr-Coulomb failure criterion [3], [4]. Thus, by obtaining a maximum shear stress, τ, (at failure) for each value of the applied normal stress, σ, a linear fit can be obtained and friction angle as well as cohesion can be inferred, as shown in Fig. 1, and expressed mathematically by (1).

$$\tau = \sigma \tan \phi + c \tag{1}$$

In addition to the direct shear test, a sinkage test will also be performed to infer the so-called Bekker parameters [2],

A. Jerves is with Division of Engineering & Applied Science, California Institute of Technology, Pasadena, CA, 91125 USA (e-mail: ajerves@caltech.edu).

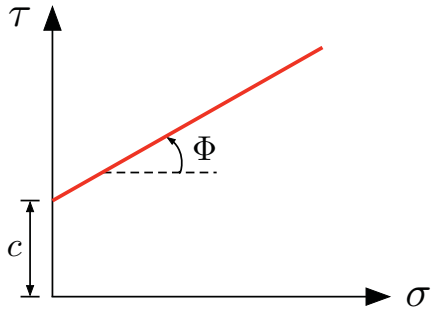

Fig. 1. Mohr-Coulomb failure criterion

[5], k and n, that satisfy the equation $\sigma = kz^n$, and where k also satisfies the Bernstein-Goriatchkin model, $k = k_c/b + k_\phi$, depicted in Fig. 2

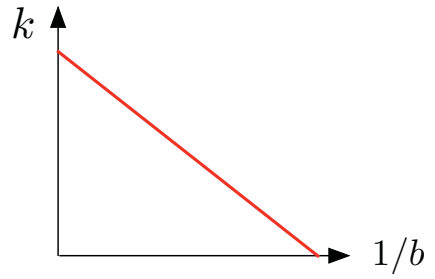

Fig. 2. Bernstein-Goriatchkin model

Thus, combining the Bekker expression and the Bernstein-Goriatchkin model, we arrive to the following expression

$$\sigma = \left(\frac{k_c}{b} + k_\phi\right) z^n$$

where b is the plate width, k_c is the cohesive modulus, k_ϕ is the frictional modulus, $k = k_c/b + k_\phi$ is the soil stiffness constant for sinkage, and n is the exponent of soil deformation. In our test, we will be measuring the sinkage, z. However, we will not have an opportunity to measure k and n for different values of b, and that is why we will not obtain k_c and k_ϕ [5] (See Appendix A).

The two components of the direct shear test that must be applied are normal stress, σ, and shear stress, τ. In a traditional laboratory setting, a sample of soil can be taken from a site and experimented on. However, in cases where this is not

possible, such as on a celestial body, a lack of resources would demand an in-situ method. The standard method for the direct shear test on a rover is described in [1]. Ridges on the rover wheels are used to create a circular failure surface rather than the traditionally linear one. While this is a space-efficient design, only the friction angle is obtained experimentally. Cohesion is obtained analytically, because of how the soil is being disturbed as the wheel sinks into position. In the case of the herein propossed device (shown in Fig. 3), cohesion and internal friction angle can both be obtained by in-situ experimentation.

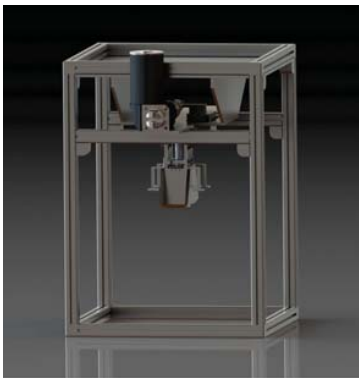

Fig. 3. Full mechanism from isometric view

The dimensions of the entire device, as seen in Fig. 3, including the external frame are 40.08 cm $\times$ 40.08 cm $\times$ 55.08 cm . However, the area being sheared is only 4.6 cm $\times$ 5.2 cm. This is due to the fact that the mentioned frame has been added to the design only for testing purposes, where it is used to provide normal stress to the prototype. Hence, the frame is not part of the prototype, and, therefore, it will not be present if the proposed device is added to a rover, or any other exploratory vehicle.

The frame consists of 4 vertical 80/20 aluminum shafts connected to each other with 8 additional beams along the top and bottom for stability, and used to guide vertically the loading plate that, at the same time, is connected to the device itself. Thus, in order to provide normal stress to the prototype, weights will be applied onto the loading plate.

On the other hand, and for testing purposes as well, the shear stress is applied through a system of rails between the loading plate and the shearing box. As the actuator pushes against the mounting bar, the shearing box will also move (see, Fig. 4). Furthermore, the shear force is measured by a load cell located at the end of the actuator (see, Fig. 5), which experiences a force when pushed against the mounting bar connecting two sliders being, at the same time, guided by a system of rails. Finally, the mentioned sliders are connected to a plate with a shaft that goes directly into the shearing device providing horizontal motion to it.

Moreover, in order to rotate the plates, a mechanism was developed that will cause the plates to open once the box has been submerged in regolith. A component will hang over the entire shearing box with 4 guiding rods, constraining it to

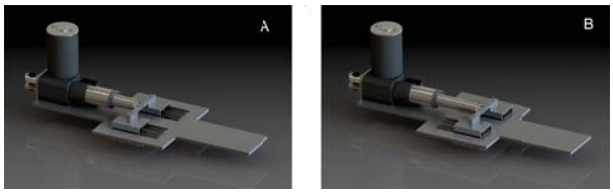

Fig. 4. A: Driving mechanism from isometric view (with actuator contracted) B: Driving mechanism from isometric view (with actuator expanded)

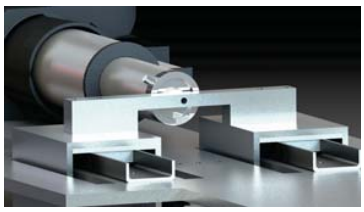

Fig. 5. Load cell mounted onto the actuator

move vertically (see, Fig. 6). The surface of regolith where the box is being submerged will push the component upwards as the entire mechanism is lowered, until it presses up against, and eventually unlocks a hinge. The two plates are secured together in an unstable equilibrium by this locked hinge, with 2 springs connecting the two plates at the top (see, Fig. 7). Once the hinge begins to open, the force of the springs will continue to pull it with enough force to clear the nearby regolith. Afterwards, the shearing mechanism will be free to move relative to the rotating plates (see, Appendix B - C).

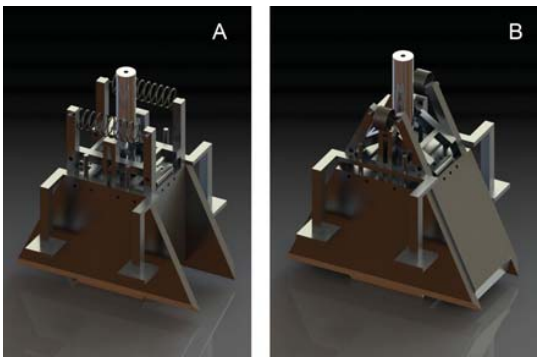

Fig. 6. A: Opening mechanism from isometric view (closed) B: Opening mechanism from isometric view (open)

Finally, we allow the shearing unit to move independently with respect to the clearing plates by a trench in the horizontal plate to which the rotating flaps are connected (see, Fig. 8). Once the clearing plates open, the shearing unit is free to move while the plates remain stationary. Once the entire mechanism is lifted out of the regolith and the plates are closed, the box will return to a default position because of the slots in the clearing plates. This design allows the mechanism to consistently perform the test many times.

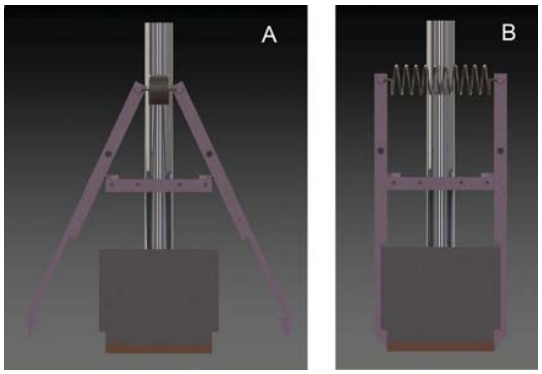

Fig. 7. A: Shearing mechanism from side view (closed) B: Shearing mechanism from side view (open)

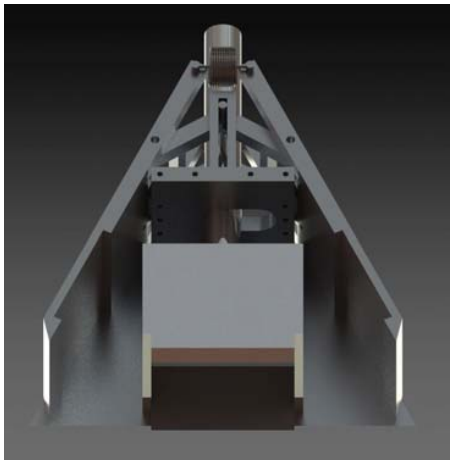

Fig. 8. Trench from below

A. Shear Test Procedure

Unfortunately, after the device was constructed, we had to implement a modified testing procedure. This changes were due to the low quality of materials used for the automated clearing unit and the limited budged/time provided for the project. Then, we decided to, at least, prove the proposed concept: "in-situ shear and sinkage tests with a small hollow shearing box". Hence, the regolith was instead cleared manually before shearing. The rest of the procedure and related equipment remained the same, and is described below step by step.

1) Compact regolith with plate under box 35 times.
2) Lower manually the loading plate while controlling horizontality with a level and using a counterweight opposite, in position, to the actuator until the box has sunk into the regolith (This, due to the lack of stability in the vertical movement, and inherent to the external frame and corresponding vertical sliders).
3) Add 15 weights (3.5 lb., each) onto the loading plate.
4) Clear carefully by hand the soil in front of the box.
5) Remove all the weights.
6) Add weights (3.5 lb., each) onto the loading plate until desired weight is achieved.
7) Run the actuator for the full length of the rails, stopping the actuator before it reaches the end.
8) Record min/max data from the oscilloscope.
9) Retract actuator.
10) Lift box out of regolith.

III. Tests and Results

Recalling, and as described in the previous sections of this document, we designed the proposed device to perform two types of tests: in-situ simple shear test, and in-situ sinkage test. As usual, the proposed model had to be built, and then tested in order to obtain and infer data that can be compared to the data from other similar well-proven procedures and equipment and for a same kind of materials. Hence, for the tests, we used Mojave Mars Simulant with particles less than 2mm in size (MMS$<$2mm), which was provided by JPL (NASA's Jet Propulsion Laboratory at the California Institute of Technology).

The results of some of the test are explained and shown in the subsections below.

A. Direct Shear Test

As shown in Fig. 9, the internal friction angle inferred from our experimental results is $50.2°$, being similar to the corresponding $46.4°$ provided by JPL for MMS $<$ 2mm.

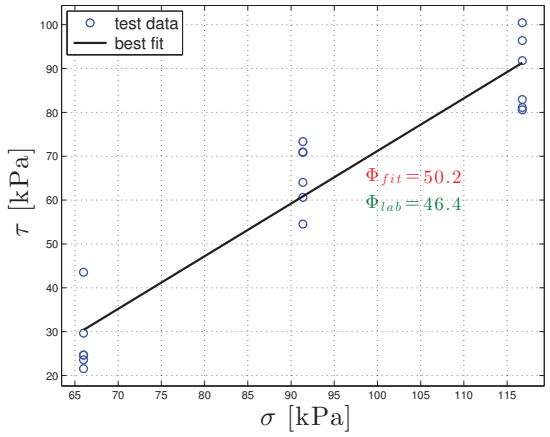

Fig. 9. Results of the in-situ simple shear test (blue circles) and corresponding best linear fit (black line)

An important aspect of our data is that the resulting cohesion is -48.82 kPa, compared to the cohesion of 3.53 kPa provided by JPL for the same simulant. The resulting error is most likely due to the fact that the normal stress is not what we believe it to be. This could be due to the fact that the frame that stabilizes the device is taking some of the load, thereby reducing the effective normal stress. However, because these experiments produce an accurate friction angle, the device works in principle, and cohesion would be obtainable with a more reliable method of applying or measuring normal stress

as, for instance, locating a load cell inside (on the upper wall) of the hollow shear box, or improving stability on the vertical motion of the device provided by the external frame for the prototype testing.

B. Force vs. Time and Force vs. Displacement

Fig. 10 A and B show how the shear force first increases in magnitude, as time evolves, before the shearing box moves. Then, once the mentioned box starts to move and shear the soil below it, note that the shear force first decreases slowly, and then stays relatively constant for the remainder of the test. This is in accordance to the kind of behavior expected from a granular (frictional/plastic) material undergoing a classical direct shear test.

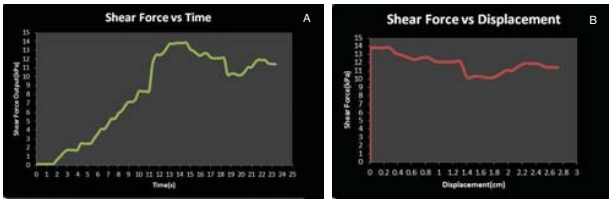

Fig. 10. A: Force vs. time graph. B: Force vs. displacement

C. Bekker Parameters

The device can also be used, as mentioned before, to perform sinkage tests in order to obtain the so-called Bekker parameters [2], [5], which are commonly used for path-planning and/or to select adequate landing sites. The results of the sinkage tests and their least squares fit to the Bekker equation, $\sigma = kz^n$, are shown by Fig. 11.

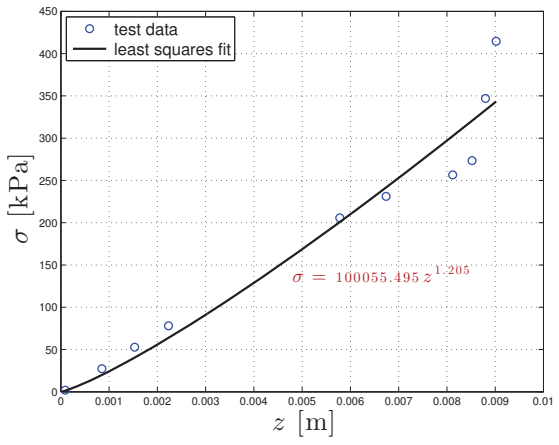

Fig. 11. Results of the sinkage test (blue circles) and corresponding fit to the Bekker equation $\sigma = kz^n$

Hence, our test results give us a soil stiffness constant for sinkage, $k = 100055.495\ kN/m^{n+2}$, as well as, an exponent of soil deformation, n=1.205. Unfortunately, so far, we have not been able to obtain official values of these parameters from JPL or any other University, laboratory, or publication, so we cannot compare our data or calibrate our experimental setup. However, this is used as a proof of concept, to show that, in fact, an in-situ sinkage test can be performed using the device herein proposed.

IV. Conclusions

With the objective of inferring regolith properties of celestial bodies, a compact and efficient device must be designed in order to accommodate for the limited space and energy disposability in a rover or exploratory vehicle. The device has been designed with the intention of performing in-situ tests on regolith or soil. While such a mechanism exists, it sacrifices accuracy for practicality. This device seeks to minimize the amount of space occupied, while still providing a higher degree of reliability in results.

The most significant problems encountered in this study were of constructive type, and due to the poor quality of the materials and procedures used to build the device. However, an improved version was designed and is presented in the videos on the website of the Keck Institute for Space Studies dedicated to this project: http://kiss.caltech.edu/study/regolith/. This improved version includes load cells placed inside of the shearing box. Additionally, a new external frame is designed for improved linear vertical motion and strain control rather than force control.

Finally, the "in-situ simple shear test" concept and device was proven, obtaining a friction angle value similar to the provided by JPL for the regolith simulant, MMS<2mm, used for the tests of the proposed prototype. Hence, the device appears to work, and with the proposed improvements more consistent and automated measurements will be possible.

Appendix A
Bekker Parameters Approximation

A. Least Squares

Let $y = f(x, b)$ be a given function. On the other hand, as a result of m observations we have a series of y_μ, x_μ values (μ=1, ... , m). Hence, we can compute:

$$\hat{y}_\mu = f(x_\mu, b)$$

Then, a vector of residuals is defined by the difference:

$$e_\mu = y_\mu - \hat{y}_\mu = y_\mu - f(x_\mu, b)$$

which, in its turn, is a function of the parameters b. Thus, the residual sum of squares (RSS) can be minimized to obtain an approximation, $\hat{b}$, of the mentioned parameters.

$$\hat{b} = \arg\min \mathrm{RSS(b)}$$

which can also be expressed as:

$$M(b) = RSS(b) = e_\mu^T e_\mu = \sum_{\mu=1}^{m} (y_\mu - f(x_\mu, b))^2$$

In the case of inferring Bekker parameters, $\sigma = z^n k$, we have

$$M(k,n) = \sum_{\mu=1}^{m} (\sigma_\mu - z_\mu^n k)^2$$

Minimizing this last expression with respect to k and n

$$\begin{cases} \sum_{\mu=1}^{m} (\sigma_\mu - z_\mu^n k) z_\mu^n = 0 \\ \sum_{\mu=1}^{m} (\sigma_\mu - z_\mu^n k) z_\mu^n \ln(z_\mu) = 0 \end{cases}$$

so, we have a system of two equations with two unknowns. Hence, we have

$$k = \frac{\sum_{\mu=1}^{m} \sigma_\mu z_\mu^n}{\sum_{\mu=1}^{m} z_\mu^{2n}}$$

and,

$$f(n) = \sum_{\mu=1}^{m} z_\mu^{2n} \sum_{\mu=1}^{m} \sigma_\mu z_\mu^n \ln(z_\mu) - \sum_{\mu=1}^{m} \sigma_\mu z_\mu^n \sum_{\mu=1}^{m} z_\mu^{2n} \ln(z_\mu) = 0$$

with corresponding first derivative given by

$$f'(n) = \sum_{\mu=1}^{m} z_\mu^{2n} \ln(z_\mu) \sum_{\mu=1}^{m} \sigma_\mu z_\mu^n \ln(z_\mu) + \sum_{\mu=1}^{m} z_\mu^{2n} \sum_{\mu=1}^{m} \sigma_\mu z_\mu^n \ln^2(z_\mu) - 2 \sum_{\mu=1}^{m} \sigma_\mu z_\mu^n \sum_{\mu=1}^{m} z_\mu^{2n} \ln^2(z_\mu)$$

Finally, since $f(n)$ is a non-liner equation with no analytical solution, we use the Newton-Raphson method to find its roots, as described in the following subsection.

B. The Newton-Raphson Method

The Newton-Raphson is a method for finding successively better approximations to the roots, $f(n) = 0$, of a real-valued function f. A first educated guess, n_0, for a root of f, starts the method. Then, the next approximation, n_1, is given by

$$n_1 = n_0 - \frac{f(n_0)}{f'(n_0)}$$

The process is iteratively repeated as:

$$n_{i+1} = n_i - \frac{f(n_i)}{f'(n_i)}$$

until an "accurate enough" value is reached. This method has quadratic convergence, as long as, the first approximation is chosen correctly enough. Otherwise, the method may fail to converge.

Appendix B
Displacement of Regolith by Rotating Panels

A. Calculation of the Force Required to Displace Regolith

External plates will first rotate to clear regolith on either side of the proposed mechanism in order to allow the shearing unit to move as shown in Fig. 7 and Fig. 12. The total amount of force required is 750.137 N or 168.638 lb. These values were calculated with the following properties:

$$\rho = 2000\ kg/m^3,\ p_{atm} = 101325\ Pa,\ g = 9.81\ m/s^2,$$

$$w = 0.0635\ m,\ h = 0.1153\ m$$

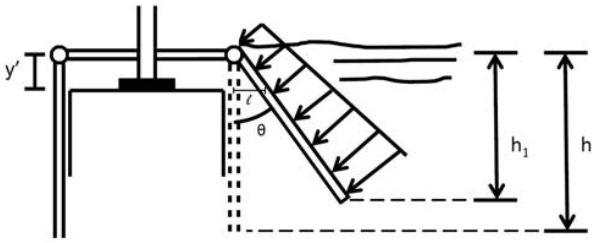

Fig. 12. Calculation of the force exerted by the regolith on the clearing plates

Also, from Fig. 12 we know that $y' = l\cot(\theta)$, and $h_1 = h\cos(\theta)$. Hence, a general expression for the force is derived

$$F = \frac{1}{2} hw\cos(\theta)\left(\rho g h\cos(\theta) + 2p_{\text{atm}}\right)$$

Appendix C
Calculation of Moment Due to Regolith

If we want to clear the regolith by rotating the clearing plates with respect to the top plate, the moment that the regolith exerts on them must be overcome. Based on our data, the length of the moment arm is 5.7862 cm.

A. Calculating the Center of Gravity of the Displaced Regolith

Finally, we compute the point at which the total force exerted by the regolith on the clearing plates is applied on them, based on the corresponding pressure prism as depicted by Fig. 13.

The point at which the total force is being applied can be computed from the following expression

$$\bar{y}_T A_T = \bar{y}_r A_r + \bar{y}_t A_t$$

where, A_T, A_r, and A_t are the areas of the total trapezoid (pressure prism), as well as, the rectangle and triangle, respectively. In the same way y_T, y_r, and y_t are

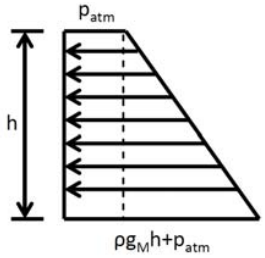

Fig. 13. Pressure prism produced by the regolith acting on the clearing walls (worst case scenario)

the centers of masses of the corresponding geometric figures. Hence, the trapezoids area is

$$A_T = \frac{(\rho g h + 2p_{\text{atm}})h}{2}$$

In the same way,

$$\bar{y}_T A_T = \frac{h}{2} h p_{\text{atm}} + \frac{h}{3}\frac{1}{2}\rho g h h$$

$$= \frac{h^2}{6}(3p_{\text{atm}} + \rho g h)$$

Hence,

$$\bar{y}_T = \frac{h}{3}\frac{3p_{\text{atm}} + \rho g h}{2p_{\text{atm}} + \rho g h}$$

But we want the arm $y'_T = h - \bar{y}_T$, so

$$y'_T = h\left(1 - \frac{1}{3}\frac{3\rho_{atm} + \rho g h}{2\rho_{atm} + \rho g h}\right)$$

Acknowledgment

This work was possible thanks to the financial support of the Keck Institute for Space Studies (KISS), and the important contributions of Dr. Brian Trease, Dr. Matt Golombek, and Dr. Julie Castillo from the NASA's Jet Propulsion Laboratory at the California Institute of Technology (JPL), who collaborated giving technical advise and providing regolith simulant (MMS<2mm) for the experimental phase of the project.

References

[1] R. Sullivan, R. Anderson, J. Biesiadecki, T. Bond, and H. Stewart. "Cohesions, Friction Angles, and Other Physical Properties of Martian Regolith from Mars Exploration Rover Wheel Trenches and Wheel Scuffs." *Journal of Geophysical Research* 116.E2 (2011): n. pag. Print.
[2] Bekker, Mieczysaw Gregory. *Theory of Land Locomotion*. Ann Arbor: Univ. of Michigan Pr. 1956. Print
[3] Das, Braja M. *Principles of Geotechnical Engineering*. Pacific Grove, CA: Brooks Cole/Thompson Learning 2002, Print
[4] Borja, Ronaldo I. *Plasticity, Modeling and & Computation*. New York, NY: Springer-Verlag/Berlin-Heidelberg 2013, Print
[5] Rashidi, Majid, and Keyvan Seyfi. "Comparative Studies on Bekker and Upadhyaya Models for Soil Pressure-Sinkage Behavior Prediction." *American-Eurasian Journal of Agricultural & Environmental Sciences*. 3.1 (2008): 19-25. Print.
[6] Bardet, Jean P. *Experimental Soil Mechanics*. Upper Saddle River, NJ: Prentice-Hall, Inc. 1997, Print